

## Scattering of 1-Mev Neutrons by Intermediate and Heavy Elements\*

M. WALT† AND H. H. BARSCHELL  
*University of Wisconsin, Madison, Wisconsin*

(Received November 27, 1953)

Differential cross sections for elastic scattering of 1-Mev neutrons from 28 intermediate and heavy elements were measured at intervals of 15° from 30° to 150°. The angular distributions of neutrons scattered by neighboring elements have similar shapes, while those of elements with appreciably different atomic weight show marked differences. For all elements forward maxima were found, and elements with atomic weight below 140 exhibited additional maxima for scattering through 180°. Maxima at about 110° were observed for elements with atomic weight near 200. From the elastic scattering cross sections, inelastic collision cross sections, and transport cross sections were obtained.

### I. INTRODUCTION

THE interaction of neutrons with nuclei has usually been described in terms of the strong interaction theory in which it is assumed that the incident neutron upon penetrating the nucleus is readily absorbed to form a compound nucleus. Since for intermediate and heavy nuclei only very limited information is available about energy states of the compound nucleus, calculations of interaction cross sections for such nuclei require the use of a method for averaging over resonances. Such averages may be obtained by employing a continuum theory.<sup>1</sup> Feshbach and Weisskopf<sup>2</sup> have calculated total interaction cross sections for fast neutrons in this manner. Their calculations based on the strong interaction hypothesis predict that total neutron cross sections averaged over resonances should decrease monotonically with energy. On the other hand, recent experiments show that the total cross sections of intermediate and heavy elements measured as a function of neutron energy exhibit broad maxima and minima which shift slowly with atomic weight.<sup>3</sup>

In order to account for these experiments Feshbach, Porter, and Weisskopf<sup>4</sup> have replaced the strong interaction hypothesis by the assumption that the incident neutron is not always absorbed into a compound system but interacts with the average potential produced by the other nucleons. The assumed potential is a complex square well of the form

$$\begin{aligned} V(r) &= -V_0(1+i\zeta), & r < R \\ V(r) &= 0, & r > R, \end{aligned} \quad (1)$$

where the imaginary part of the potential represents absorption corresponding to compound nucleus formation. With values of  $R = 1.45A^{1/3} \times 10^{-13}$  cm,  $V_0 = 19$  Mev, and  $\zeta = 0.05$  for the three parameters of the theory, calculated total cross sections are in good agreement with experimental results for neutron energies up to

3 Mev and for elements heavier than iron. The broad maxima and minima in the curves of total cross section as a function of energy and the systematic variation of these curves with atomic weight are reproduced by the theory.

In the theory of Feshbach, Porter, and Weisskopf the neutrons which pass through the nucleus without being absorbed produce a refracted wave which interferes with the incident and the diffracted wave. The angular distributions of elastically scattered neutrons calculated using the complex potential are, therefore, different from those obtained on the basis of the strong interaction model, so that measurements of angular distributions should afford a test of the theory.

Experimental data on the differential cross sections for elastic scattering have previously been published for some neutron energies between 0.2 Mev and 14 Mev.<sup>5-11</sup> In most of these experiments maxima in the forward direction were observed and in some cases additional maxima at larger angles were found. Comparison of the available results with calculated distributions is difficult, however, because either the number of scattering angles employed in the experiments was not sufficient to obtain complete angular distributions or because the detector used did not discriminate adequately against inelastically scattered neutrons.

In the present investigation angular distributions of elastically scattered neutrons were measured for a large number of elements so that one could observe both the shape of the distribution and any systematic change with atomic weight. The quantity measured directly was the cross section for elastic scattering through a given angle per unit solid angle. From a knowledge of this cross section and the total cross section it is possible to deduce the inelastic collision cross section and the transport cross section. The

<sup>5</sup> T. Wakatuki, Proc. Phys.-Math. Soc. Japan **22**, 430 (1940).

<sup>6</sup> H. H. Barschall and R. Ladenburg, Phys. Rev. **61**, 129 (1942).

<sup>7</sup> Amaldi, Bocciarelli, Cacciapuoti, and Trabacchi, Nuovo cimento **3**, 203 (1946).

<sup>8</sup> Barschall, Battat, Bright, Graves, Jorgensen, and Manley, Phys. Rev. **72**, 881 (1947).

<sup>9</sup> A. Langsdorf, Phys. Rev. **80**, 132 (1950).

<sup>10</sup> E. T. Jurney and C. W. Zabel, Phys. Rev. **86**, 594 (1952).

<sup>11</sup> W. D. Whitehead and S. C. Snowdon, Phys. Rev. **92**, 114 (1953).

\* Work supported by the U. S. Atomic Energy Commission and the Wisconsin Alumni Research Foundation.

† U. S. Atomic Energy Commission predoctoral fellow. Now at Los Alamos Scientific Laboratory.

<sup>1</sup> H. A. Bethe, Phys. Rev. **57**, 1125 (1940).

<sup>2</sup> H. Feshbach and V. F. Weisskopf, Phys. Rev. **76**, 1550 (1949).

<sup>3</sup> H. H. Barschall, Phys. Rev. **86**, 431 (1952).

<sup>4</sup> Feshbach, Porter, and Weisskopf, Phys. Rev. **90**, 166 (1953).

inelastic collision cross section is given by

$$\sigma_{in} = \sigma_T - \int \sigma(\theta) d\omega,$$

where  $\sigma_T$  is the total cross section,  $\sigma(\theta)$  the differential elastic cross section for scattering through an angle  $\theta$ , and  $d\omega$  the solid angle between  $\theta$  and  $\theta + d\theta$ . The transport cross section is of interest for some practical applications of diffusion theory and is defined by

$$\sigma_{tr} = \sigma_T - \int \sigma(\theta) \cos\theta d\omega$$

under the assumption that the inelastic scattering is isotropic.

## II. EQUIPMENT

A top view of the experimental arrangement is shown in Fig. 1. One-Mev neutrons produced by bombarding a lithium target with 2.7-Mev protons were scattered by a cylindrical sample. Scattered neutrons were observed with a detector which could be moved to various positions on an observation circle in the plane of the figure. The detector was shielded from the neutron source by a paraffin wedge.

A recoil proportional counter, biased to discriminate against inelastically scattered neutrons, was used as the detector. The neutron scattering resonance in helium at about 1 Mev favored the choice of helium as a counter gas and the use of 1-Mev neutrons for the measurements. The maximum in the total cross section at the resonance improved the counting efficiency, and as the angular distribution of 1-Mev neutrons scattered by helium is strongly peaked in the backward direction, a large fraction of the recoiling helium nuclei had close to the maximum possible energy. Below 1 Mev both the total cross section of helium and the differential cross section for scattering at  $180^\circ$  decrease rapidly with decreasing neutron energy, so that the sensitivity of the detector for room-scattered background neutrons was considerably less than the sensitivity for 1-Mev neutrons.

The counter was cylindrical with a 1.9-cm diameter outer wall and a 0.005-in. center wire, 6 cm long. It was operated in the proportional region at a pressure of 17 atmos of helium and a center wire voltage of

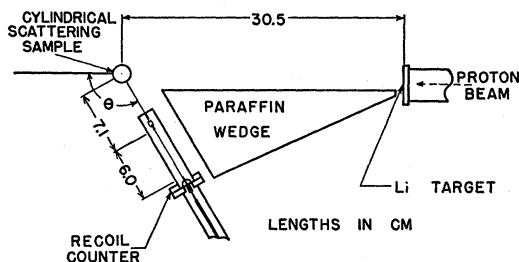


Fig. 1. Top view of the experimental arrangement.

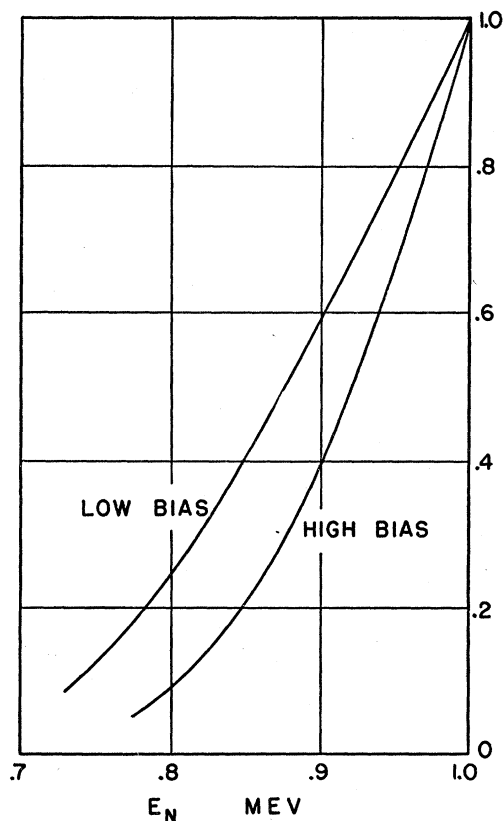


Fig. 2. Counting efficiency of the recoil detector for neutrons of energy  $E_n$  divided by the counting efficiency for 1-Mev neutrons.

1700. Pulses from the counter were amplified and fed into two scalars operated in parallel. The discriminators of the two scalars were biased to reject pulses produced by neutrons with energy below about 750 kev and 850 kev, respectively. The energy sensitivity of the counter, obtained by comparing its counting rate with the counting rate of an energy insensitive long counter<sup>12</sup> at several neutron energies, is shown in Fig. 2 where the efficiency relative to the efficiency for 1-Mev neutrons is plotted as a function of neutron energy. At energies below 1 Mev the counter efficiency was different at the two biases, so that the presence of an appreciable number of inelastically scattered neutrons with energies above 750 kev could be recognized by a difference in the values of the cross sections measured at the two biases.

Since the experimental cross sections of intermediate and heavy elements can be easily compared with theory only if the cross sections are averaged over resonances, the lithium target thicknesses were made greater than the spacing between resonances in the elements studied. Four lithium targets, with thicknesses between 90 kev and 160 kev for 2.7-Mev protons, were used during the experiment. Each target was evaporated onto a

<sup>12</sup> A. O. Hanson and J. L. McKibben, Phys. Rev. 72, 673 (1947).

tantalum backing in the target chamber shortly before use.

The scattering samples were cylinders, about 6 cm long, with diameters varying from 1.25 cm to 2.7 cm, depending upon the total cross section of the element and the number of nuclei per cubic cm. The diameter of each sample was chosen so that all samples had comparable multiple scattering. In Table I are listed the dimensions of the samples, the number of nuclei per cubic cm, and a multiple-scattering parameter  $M$  which is the fraction of the detected neutrons which were scattered at least twice before reaching the detector. With the exception of the mercury scatterer which consisted of liquid mercury in a thin-walled aluminum container, all samples were in solid, elemental form.

### III. PROCEDURE

The differential cross section for elastic scattering at an angle  $\theta$  may be determined by observing the counting rate of the detector for three experimental arrangements: (A) with the detector at angle  $\theta$  and the scatterer in place; (B) with the detector at  $\theta$  but with the scatterer removed; and (C) with the detector in the position normally occupied by the scattering sample. The shielding wedge remained in position in all three cases. For thin samples the cross section is then given by

$$\sigma(\theta) = (A - B)d^2/CN, \quad (2)$$

where  $A$ ,  $B$ , and  $C$  are the counting rates for a constant neutron source strength, observed in the three experimental arrangements, (A), (B), and (C).  $N$  is the total number of scattering nuclei, and  $d$  is the distance from the scattering sample to the counter.

Counting rates for the three conditions were measured by recording the number of counts obtained in a run during which a fixed number of neutrons was produced at the source. Each of these runs lasted about two minutes and was controlled by a current integrator which ended the run when a fixed proton charge was accumulated at the lithium target. The data were taken in many short runs, the three different arrangements being used in successive runs, so that gradual changes in the target yield or the counter sensitivity would be averaged out. Enough runs were taken at each scattering angle to give a statistical error of about 5 percent in the cross section.

Measurements were made at  $15^\circ$  intervals for angles from  $30^\circ$  to  $150^\circ$ . The background, i.e., the counting rate with the sample removed compared to the counting rate with the sample in place, averaged about 40 percent but depended upon the scattering angle and the scattering element. At  $150^\circ$ , where the shielding was limited by the available space between the counter and source, the background for some elements was as high as 80 percent.

As it was easier to place the counter at  $0^\circ$  on the observation circle rather than in the sample position

to observe the direct beam in the arrangement (C), the counting rate measured on the observation circle was multiplied by a constant to give the value which would have been measured at the sample position. This constant was determined experimentally by observing the counting rates with the detector in each of the two positions.

In formula (2) it was assumed that the counter detected primary and scattered neutrons with equal efficiency. The rapid decrease in counting efficiency with decreasing neutron energy resulted, however, in a lower sensitivity for detecting elastically scattered neutrons which had lost some energy in the laboratory system. In addition, the sensitivity of the counter depended on the counting rate. As a result, the direct and scattered neutrons were detected with different efficiency, since the direct flux was 50 to 100 times greater than the flux of scattered and background neutrons. Correction for the energy loss in elastic collisions was made by calculating the energy of the scattered neutrons and using the energy sensitivity of the counter shown in Fig. 2. To estimate the counting-rate effects the counter was placed in the direct beam and the number of counts per run was recorded at two proton currents which produced counting rates roughly equal to those encountered in measuring the direct and the scattered flux. Since the number of neutrons produced during each run was constant, the effect of counting rate upon detector sensitivity was shown by a difference in the number of counts registered during the two runs. The results of this test indicated that the efficiency of the detector decreased by 10 percent in the higher flux.

The distance  $d$  in formula (2) was obtained directly by experiment to avoid the necessity of knowing the variation of the sensitivity over the active volume of the counter. At a distance of about 35 cm from the source the lower sensitivity at the ends of the center wire had little effect on the average distance, since the length of the active volume was small compared to the distance from the source. The number of counts per run was recorded with the counter 35 cm from the source and with the counter at a distance from the source equal to its distance from the axis of the scatterer during the cross section determinations. By assuming that the counts per run varied inversely with the square of the distance from counter to source, the value of  $d$  was found. The proton current was adjusted to give the same flux at each of the two distances in order to avoid the counting-rate effects mentioned in the preceding paragraph.

Formula (2) is valid only for thin samples for which there is negligible attenuation of the primary beam and negligible multiple scattering. To correct for the attenuation of the primary beam the ratio of the average flux within the sample to the incident flux was computed, and the measured direct counting rate  $C$  was

multiplied by this ratio to give an average value of  $C$  within the sample.

As the diameters of the scattering samples were about  $\frac{1}{2}$  of a mean free path for scattering, some of the scattered neutrons were scattered again before leaving the sample. These multiple-scattering processes tended to diminish the maxima and raise the minima in the angular distributions, so that the observed scattering was more isotropic than the true differential cross section. The procedure followed in computing the correction for this multiple scattering was to assume an initial curve for the differential cross section, then calculate the results of an experiment performed on a scattering sample with the assumed cross section. By adjusting the initial curve until the calculated result coincided with the experimentally measured distribution, the corrected values of the differential cross section were obtained.

To compute the result of an experiment on a sample with a given differential cross section, the following simplifying assumptions were made: (1) no neutron made more than three collisions in the sample; (2) the fraction of the doubly scattered neutrons which suffered a third collision was the same as the fraction of singly scattered neutrons which suffered a second collision; (3) the angular distribution of doubly and triply scattered neutrons leaving the sample was the same as the distribution of doubly and triply scattered neutrons in an infinite medium of the sample material. Methods for computing second- and third-collision distributions in infinite media from a knowl-

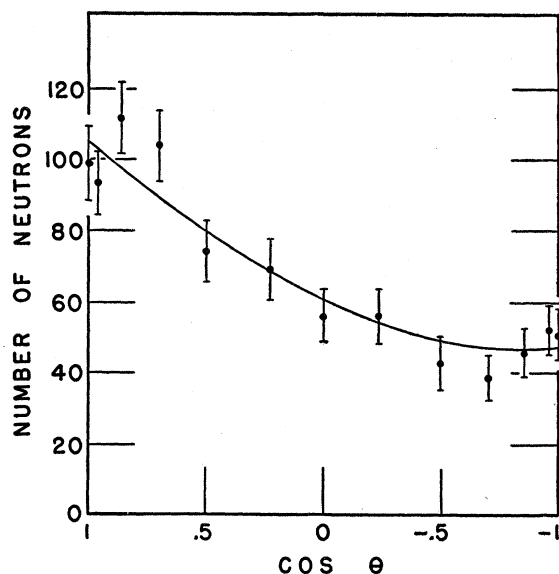


FIG. 3. Check of simplifying assumption used in multiple scattering correction. The circles give the distribution of neutrons reaching the detector after two collisions as obtained by the Monte Carlo calculation. The solid line indicates the distribution of doubly scattered neutrons in an infinite medium of the scattering material.

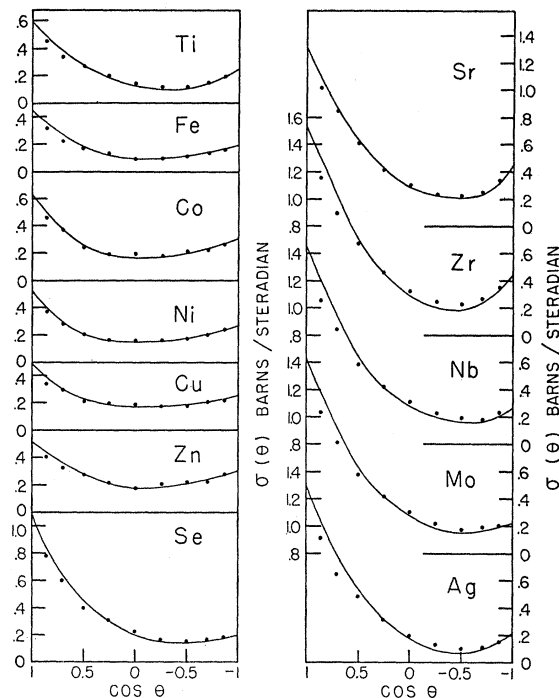


FIG. 4. Differential cross sections for elastic scattering of 1-Mev neutrons from Ti, Fe, Co, Ni, Cu, Zn, Se, Sr, Zr, Nb, Mo, and Ag. The circles give experimental values before the correction for multiple scattering. The solid line is the differential cross section after correction for multiple scattering.

edge of the first-collision distributions have been published by several authors.<sup>13,14</sup>

These simplifying assumptions were checked by performing a Monte Carlo calculation on a typical example. About 15 000 scattered neutrons were tracked through a sample having the properties of cadmium. The nature of the event at each step in the path through the sample was selected in sequence from the existing possibilities, each possibility being weighted according to its probability of occurrence. The most critical of the aforesaid assumptions was that the distribution of second-collision neutrons entering the detector was the same as the distribution of second-collision neutrons in an infinite medium. That this assumption does not introduce any large error can be seen from Fig. 3 where the distribution of the second-collision neutrons obtained by the Monte Carlo example is shown with the distribution of second-collision neutrons in an infinite medium. Additional information from the Monte Carlo work indicated that only very small errors are introduced by the other assumptions.

#### IV. RESULTS

Figures 4 to 6 give the differential cross sections for elastic scattering of 1-Mev neutrons by titanium, iron, cobalt, nickel, copper, zinc, selenium, strontium,

<sup>13</sup> S. Goudsmit and J. L. Saunderson, *Phys. Rev.* **57**, 24 (1940).

<sup>14</sup> J. Blok and C. C. Jonker, *Physica* **18**, 809 (1953).

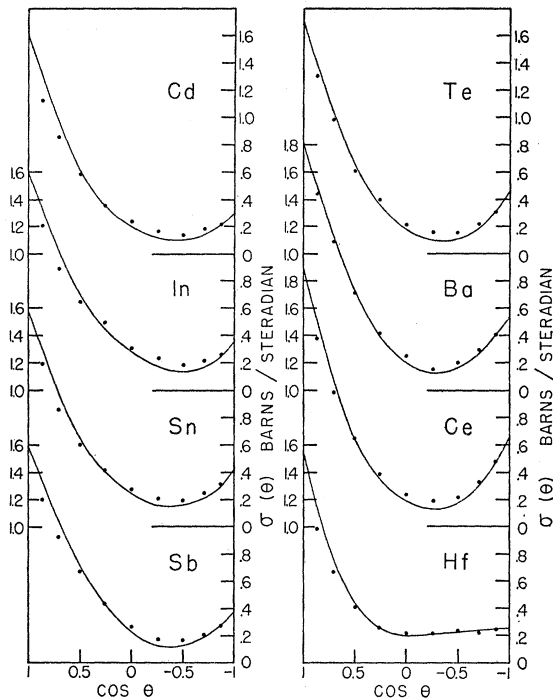


FIG. 5. Differential elastic cross sections of Cd, In, Sn, Sb, Te, Ba, Ce, and Hf.

zirconium, niobium, molybdenum, silver, cadmium, indium, tin, antimony, tellurium, barium, cerium, hafnium, tantalum, wolfram, gold, mercury, radiogenic lead (88 percent  $Pb^{206}$ ), lead, bismuth, and thorium. The circles give the experimental cross sections uncorrected for multiple scattering and the solid lines give the values of the differential cross sections after the correction for multiple scattering was made. The differential cross sections are plotted as a function of the cosine of the scattering angle, since at 1 Mev it is expected that partial waves of high angular momenta are not involved and that the curves should, therefore, have simpler forms if plotted in this manner. Cross sections for both biases are plotted for wolfram since the results obtained at the two biases did not agree, the higher bias giving the smaller differential cross section. This effect was attributed to the presence of inelastically scattered neutrons with energies greater than 750 kev. The lack of bias effect in all elements except wolfram indicates that the inelastically scattered neutrons lost at least 250 kev in the collision. This might be expected since most of the elements studied do not have known excited states below 250 kev.<sup>15</sup> On the other hand the first excited state of wolfram is at about 100 kev for the isotopes with 106, 108, and 112 neutrons.

From the curves of Figs. 4 to 6 and from previously

<sup>15</sup> G. Scharff-Goldhaber, Phys. Rev. **90**, 587 (1953).

measured values of the total cross sections,<sup>16-18</sup> the inelastic collision cross sections and the transport cross sections were obtained. In cases where the total cross section varied rapidly with energy near 1 Mev, the transmission measurements were repeated with the lithium target used for the differential cross section experiment to obtain proper averaging over resonances.

The inelastic collision cross sections and the transport cross sections are given in the last two columns of Table I. The lower curve of differential cross section was used to determine the inelastic cross section of wolfram, but since it is possible that inelastically scattered neutrons were detected even with the higher bias, the value of the inelastic collision cross section is only a lower limit.

The over-all error in the differential cross section is about 15 percent for angles between 30° and 150°. The principal uncertainties contributing to this are: statistical errors, 5 percent; the error in the correction for loss of counter sensitivity in the direct flux, estimated to be not more than 5 percent; and the errors in the distances involved in the cross-section determination, 5 percent. The errors in the inelastic collision cross sections are about 15 percent of the value of the integral of the differential elastic cross section, since the error in the total cross section is negligible. As a large part

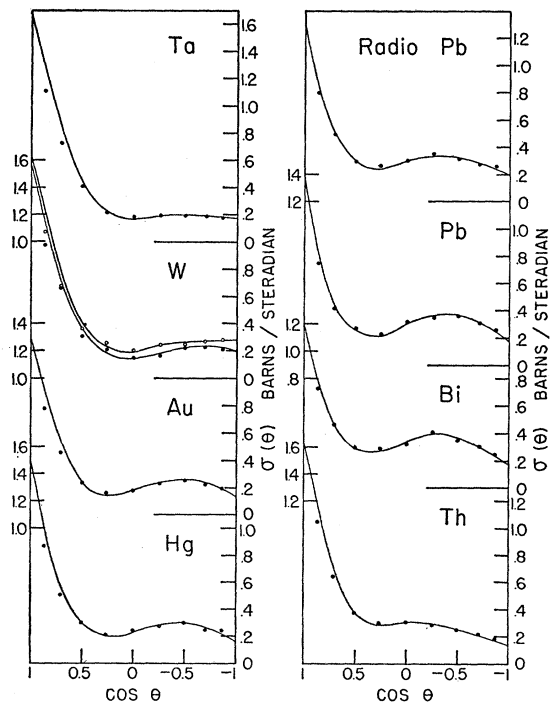


FIG. 6. Differential elastic cross sections of Ta, W, Au, Hg, Radio-lead, Pb, Bi, and Th.

<sup>16</sup> Miller, Adair, Bockelman, and Darden, Phys. Rev. **88**, 83 (1952).

<sup>17</sup> Walt, Becker, Okazaki, and Fields, Phys. Rev. **89**, 1271 (1953).

<sup>18</sup> Okazaki, Darden, and Walton, Phys. Rev. **93**, 461 (1953).

of this error is common to all elements, the relative values of the inelastic collision cross sections of different elements are, however, probably more accurate than the absolute values. The errors in the transport cross section cannot be easily estimated because the extrapolated values of the differential cross section at angles less than  $30^\circ$  and greater than  $150^\circ$  are heavily weighted in the determination of the transport cross sections.

Previous measurements of angular distributions of elastically scattered neutrons can be compared only qualitatively with the results of the present experiment, because either the energy at which the other investigations were made was higher or the angular and energy resolution was considerably different. Other investigators have observed forward maxima, and Jurney and Zabel<sup>10</sup> as well as Whitehead and Snowdon<sup>11</sup> have found additional maxima at larger angles.

The most extensive measurements of inelastic collision cross sections in this energy region are those of Carter and Beyster,<sup>19</sup> who used fission neutrons and threshold fission detectors. Again the energy was sufficiently different from that used in the present measurement to prevent detailed comparison, but certain features are brought out in both experiments. There is a tendency, more noticeable in the work of Carter and Beyster than in this experiment, for the inelastic cross sections of magic number nuclei to be lower than those of their nonmagic neighbors. Table I corroborates this tendency for bismuth, lead, radiogenic lead, cerium, and barium, although the inelastic cross sections of strontium and tin are not especially low. The fact that no known excited states of the principal isotopes of Sr and Sn occur below 1 Mev might suggest that their inelastic cross sections should be lower than the values given in Table I.

Previous measurements of transport cross sections are in good agreement with the values of Table I. In reference 8 the transport cross sections were reported at energies of 0.6 Mev and 1.5 Mev for Fe, Co, Cu, W, and Pb. For all elements except W the values in Table I lie between those given in the reference.

## V. DISCUSSION OF RESULTS

The most outstanding feature in the results of the present measurements is the similarity in the angular distributions of elements which have nearly the same atomic weight. This behavior is clearly shown in Fig. 7 where the differential cross sections of all the elements investigated are presented in order of atomic weight. Theoretical angular distributions based on continuum theories using either the strong interaction hypothesis<sup>2</sup> or the complex potential proposed by Feshbach, Porter, and Weisskopf<sup>4</sup> also show the slow variation with atomic weight, since only parameters which change slowly with nuclear size appear in the continuum formulations.

<sup>19</sup> R. E. Carter and J. R. Beyster, Phys. Rev. **90**, 389 (1953).

TABLE I. Properties of scattering samples and values of inelastic collision cross sections and transport cross sections.

Element	Radius cm	Length cm	Nuclei per $\text{cm}^3 \times 10^{-23}$	$\sigma_T^a$	$M$	$\sigma_{in}$	$\sigma_{tr}$
Ti	1.194	6.04	0.566	2.9	0.16	0.1	2.1
Fe	1.260	5.99	0.847	2.5	0.20	0.4	2.1
Co	1.168	6.10	0.703	3.5	0.21	0.2	3.0
Ni	0.952	6.02	0.914	2.9	0.19	0.1	2.5
Cu	1.102	6.08	0.845	3.2	0.21	0.3	2.8
Zn	1.115	6.02	0.657	3.6	0.20	0.3	3.3
Se	1.23	6.26	0.310	5.0	0.16	0.7	3.5
Sr	1.11	5.46	0.180	6.7	0.12	0.7	4.8
Zr	0.953	6.08	0.430	7.0	0.21	0.4	4.6
Nb	0.870	6.35	0.491	6.5	0.20	0.7	4.2
Mo	0.788	6.15	0.635	6.8	0.23	1.1	4.6
Ag	0.890	6.02	0.587	6.6	0.23	2.1	4.4
Cd	0.940	6.02	0.463	6.9	0.22	1.4	4.4
In	1.110	6.06	0.386	6.6	0.21	0.4	4.1
Sn	1.269	6.06	0.369	6.8	0.22	0.7	4.6
Sb	1.182	6.11	0.328	7.0	0.20	0.8	4.4
Te	1.276	6.40	0.250	6.5	0.17	0.6	3.9
Ba	1.235	6.13	0.151	6.8	0.11	0.2	4.3
Ce	1.265	6.08	0.287	6.8	0.19	0.1	4.4
Hf	1.270	4.44	0.448	7.2	0.25	2.1	5.4
Ta	0.635	6.05	0.552	7.3	0.19	2.2	5.2
W	0.635	6.15	0.637	6.9	0.21	$\geq 2.2$	5.3
Au	1.270	6.17	0.596	5.6	0.25	1.5	4.4
Hg	1.160	6.10	0.408	5.6	0.20	0.9	4.3
Pb <sup>206</sup>	1.345	6.00	0.330	4.9	0.17	0.2	4.0
Pb	1.350	6.08	0.330	4.9	0.17	0.3	4.1
Bi	1.345	6.02	0.283	4.9	0.15	0.1	4.1
Th	1.268	6.04	0.300	7.1	0.20	1.8	5.3

<sup>a</sup> See references 16, 17, 18.

A comparison of the measured elastic cross sections with calculations is complicated by the fact that at a neutron energy as low as 1 Mev there is an appreciable probability for the decay of the compound nucleus by elastic scattering. In particular, if the bombarded nucleus has no energy level below 1 Mev, as is probably the case for several of the elements investigated, most of the compound nucleus formation will result in elastic scattering. This "compound-elastic" scattering cannot be distinguished experimentally from the "shape-elastic" scattering which is not associated with compound nucleus formation, but the "compound-elastic" scattering is expected to have a different angular distribution from the "shape-elastic" scattering. It is possible to calculate from the theory the cross section for formation of a compound nucleus, but not what fraction of the compound nuclei decays by elastic or inelastic processes. Consequently, only the limits between which the elastic scattering and inelastic collision cross sections should lie can be predicted.

While all the inelastic collision cross sections listed in Table I are smaller than the maxima calculated on the basis of the strong interaction theory, some of the values appear to be larger than the upper limits calculated using the complex potential (1), but the large errors in the experimental values overlap the limits.

If the inelastic collision cross sections were known accurately from the experiments, it would be possible to calculate from the theory definite angular distributions for the elastic scattering. Because of the un-

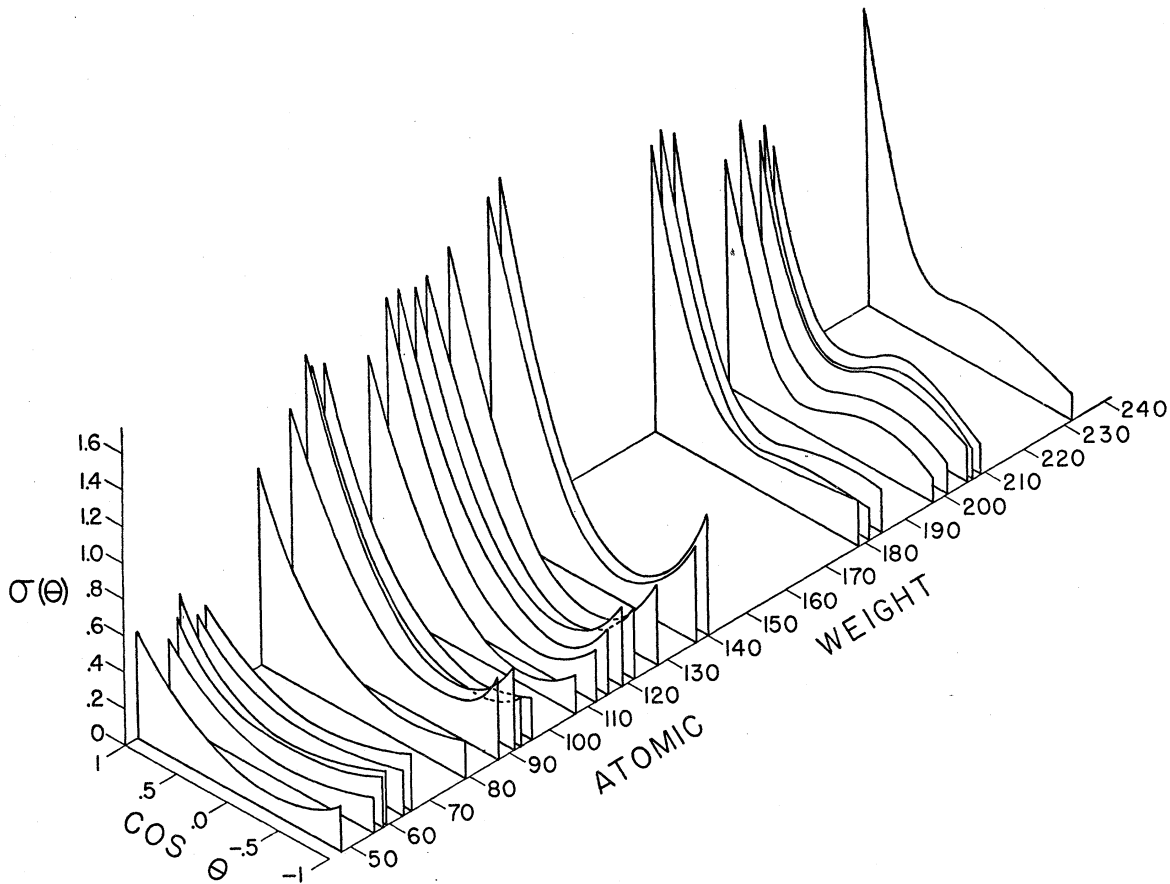


FIG. 7. Differential cross section for elastic scattering of 1-Mev neutrons as a function of the cosine of the scattering angle and of atomic weight.

certainty in the values for the inelastic cross section, however, it is not known how much "compound-elastic" scattering should be added to the calculated angular distributions of "shape-elastic" scattering. Certain characteristic features of the predicted angular distributions are independent of the assumed amount of "compound-elastic" scattering. Distributions calculated on the basis of the strong interaction model<sup>20</sup> have pronounced maxima at  $0^\circ$  in agreement with experiments. This theory does not predict, however, additional maxima at  $110^\circ$  of the magnitude encountered in the heavy elements. On the other hand, the observed maxima at  $180^\circ$  for elements of atomic weight below 160, and maxima around  $110^\circ$  for elements of atomic weight near 200 are characteristic features

of the angular distributions calculated from the complex potential (1).<sup>21</sup>

While it is not possible to state that the experiments are definitely in agreement with the recently developed theory of Feshbach, Porter, and Weisskopf, the results appear to agree better with this theory than with the compound nucleus theory.

#### VI. ACKNOWLEDGMENTS

We wish to thank Professor P. C. Hammer and Mr. J. W. Hollingsworth for coding the Monte Carlo example and performing the calculations on the I.B.M. 604 Card Programmed Calculator. We are grateful to Professor V. F. Weisskopf for valuable discussions and for making the results of reference 21 available to us before publication.

<sup>20</sup> Final Report of the Fast Neutron Data Project, 1951, Atomic Energy Commission Report NYO-636 (unpublished).

<sup>21</sup> Feshbach, Porter, and Weisskopf, Technical Report No. 62, Laboratory for Nuclear Science, Massachusetts Institute of Technology, Cambridge, Massachusetts, 1953 (unpublished).